 doi:10.20944/preprints202203.0045.v1

Article

Morphotectonic and petrological characteristics of Permo-Triassic traps of Siberia

Victor Sharapov [1,*], Yury Perepechko [1], Anna Mikheeva [2], Igor Ashchepkov [1], Viktoria Lyamina [1] and Anatoly Boguslavsky [1]

1 Sobolev Institute of Geology and Mineralogy, Siberian Branch of the Russian Academy of Sciences Novosibirsk;Russia; vik@igm.nsc.ru (V.S.); yuri@perep.ru (Y.P.); garnet@igm.nsc.ru (I.A.); balandis@igm.nsc.ru (V.L.); boguslav@igm.nsc.ru (A.B.)
2 The Institute of Computational Mathematics and Mathematical Geophysics Siberian Branch of the Russian Academy of Sciences, Novosibirsk; Russia; anna@omzg.sscc.ru
* Correspondence: vik@igm.nsc.ru

Abstract: The article reports morphotectonic and petrological characteristics of magmatic systems of Permo-Triassic traps in the sedimentary cover of the Siberian Craton, Taimyr, as well as in the crystalline basement of the Mesozoic cover of the West Siberian Plate and the Kara sedimentary basin based on the relief analysis, seismotomography data, magnetic and gravitational anomalies. Four development sectors of magma-permeable zones were distinguished along the perimeter of the craton of the Anabar Shield. The western sector is characterized by an extensive stretching area, on which the lava region of volcanic ridges junction of the Tunguska syncline formed. A striking feature of subaerial volcanism is the meridional petrochemical trend of increasing the silica of basic magmas in intrusive rocks of the Siberian Craton while the volumes of embedded melts are reduced.

Keywords: Siberian traps; petrology; morphotectonics; GIS technologies

1. Introduction

From the beginning of the last century, the problem of large igneous provinces (LIPs) has been discussed in the petrology of volcanic rocks. Permo-Triassic traps of Siberia (PTTS) have the wide scale and varieties of structure and petrology, unique metallogeny on the Siberian Craton and Taimyr. To understand the nature of the traps, it is important to identify the geological boundaries and manifestation forms of igneous processes on the surface and in the sedimentary cover of the Siberian Craton (SC), West Siberian Plate (WSP) and Taimyr Peninsula (TP). Unique scales of such LIP served as a hypothesis of anomalous characteristics of the upper mantle state under the northern Asian supercontinent as the main reason for its formation [1]. In the formation of continental traps, the development of crustal spreading may take place before the opening of ocean basins by the rift formation mechanism [2]. However, in the case of PTTS, diffused spreading and subsidence of crust of WSP during the melting of the lithospheric mantle and after magmatic processes occurred without a significant reduction in its thickness [3]. A common geodynamic model for the PTTS formation [4] is the mantle hotspot pattern [5]. A model of the thermochemical superplume beneath the lithospheric plate, which melts the earth's mantle from the outer core to the lithosphere and spreads hundreds and thousands of kilometres or penetrates the lithosphere to form a threefold rift juncture of plates was proposed in [6,7]. In these models, the structural conditions for the development of magmatic systems in the crust are explained by the formation of rifts [8,9] with volcanic manifestations overlapped by the thickness of Mesozoic petroleum deposits. Outside the Mesozoic petroleum basins, on the Siberian Craton, the PTTS igneous rocks are not associated with classical rifting. A solution to this geodynamic collision can be obtained based on an analysis of the characteristics of regional and local igneous structures in the platform case, as

 doi:10.20944/preprints202203.0045.v1

well as the scale of the development of facies of igneous systems throughout the PTTS development area.

2. Methods of Analysis of the PTTS Formation

Models of the PTTS formation are discussed based on the generation pattern of mafic melts and deformation of the earth's crust by upper mantle plumes. For intraplate geodynamic processes with the formation of faults in lithospheric rocks, the sources of such deformations can be global and local stretching of the lithosphere affected by convective flows in the upper mantle, both with and without the formation of decompression melting regions [10-11]. By numerical modelling of the rift formation above asthenosphere zones for areas of slow-spreading ridges [12] and the evolution of upper mantle plumes under the WSP and SC lithosphere [13-15], we calculated lateral dimensions of rift valleys over ascending convective flows above hot spots as the first tens of kilometres by model [5]. The manifestation of mantle thermochemical plumes in the presence of a phase boundary between mantle reservoirs [16] in the studied model of hot spots coincided with the sizes of asthenosphere zones. No significant differences in the development of rifting processes associated with mantle and local upper mantle plumes were observed. Therefore, the consistency of the models should be evaluated using instrumental data records in the geodynamic interpretation of the PTTS nature.

The genetic models of PTTS origin and development can be based on the analysis of the observed intraplate mafic volcanism in Africa, Iceland and Hawaii. The structural characteristics of SC are discovered by mapping and drilling during the search and exploration of ore and petroleum deposits. Since, according to [17], Taimyr and SC by the time of PTTS formed were a single platform, signs of classical rifts are difficult to find on the SC territory. The assumed joint structure of the Khatanga and Ob rift zones in the formation of PTTS should develop followed by volcanic manifestations of traps when the volcano-plutonic systems are formed. Two almost parallel rifts were identified [18-19] on the area of WSP downfolds filled with Mesozoic and Quaternary sedimentary rocks. In [20] considered all post-Paleozoic igneous events of the Russian sector of Asia were considered as rifting processes, although there are no signs of classical rifts of the PTTS igneous systems in the described structural forms of the magma development in the sedimentary cover and subaerial mantle flows for SC and Taimyr [21-29]. The described manifestations of subaerial volcanism beneath the Mesozoic cover on the WSP territory [30-33] also do not contain geological and structural information about morphological structures common for classical rifting, therefore morphological structures characteristics of the PTTS manifestation of terrestrial magmatism should be studied by instrumental techniques.

The most meaningful methods for identifying regional features of PTTS intraplate basic magmatism are structural analysis of gravitational and magnetic anomalies [34-36] and seismic tomography [36-37]. Analysis showed that after the PTTSs formation, basic lavas were observed in the northeast and east of their development [37-38]. Most of the magnetic and gravitational anomalies in the platform Paleozoic cover of the SC and Taimyr were induced by volcanic and subvolcanic igneous trap bodies. In the eastern Anabar shield and the west Lena aulacogen, an overlap of manifestations of Middle Paleozoic and Permo-Triassic traps in faults, which contain the diamondiferous volcanic pipes, was revealed [25,40].

This paper focuses on local data of structural control of trap magmatism in the SC Paleozoic platform cover and under the WSP Mesozoic cover obtained using GIS technologies [41-43] and supplemented by the analyses of the regional magmatism of SC and WSP, conducted in [34-36] and the forms of volcanic edifices and fractures of the earth's crust in the PTTS manifestation. Seismotomographic data visualization was carried out using an original data processing system GIS-ENDDB [43-44]. The system uses a tomographic model "SL2013sv" on a transverse SV-wave with vertical polarization [45] containing values of velocity deviations from the basic velocity SV0 by 28 depth levels to H =

700 km. The selected seismotomography method has good sensitivity to rheological discontinuities in the earth's crust and better depth resolution. The obtained digital model has a step of 0.5° by lateral and 25 km by depth, the accuracy of SV velocity deviation from the basic one is 0.001%. Visualization of local gravitational anomalies was also conducted via the GIS-ENDDB software system [41,43] using a shadow-gravity model of the anomalies field according to the data of "Global marine gravity" (model V18.1 [46] with a resolution for the water body: 30″ per a point by latitude λ, and cos (φ)· 30″ by longitude λ; and for onshore: 1′ (min) per point by φ, and cos (φ) 1′ by λ). The data sources for this model are the altimetric missions of ERS-1 and Geosat/GM, and the global model - Earth Gravitational Model (EGM-2008) prepared by the US National Geospatial-Intelligence Agency NGA, including Russian surface mapping data [46-47]. For clear identification of tectonic and structural zones in GIS-ENDDB, the initial gravitational field was recalculated into local anomalies by extracting the local component background by the Andreev-Griffin variation method using anti-aliasing (moving circle averaging of a given radius R) and subtracting the obtained value from the observed field.

3. PTTS Magma System Manifestations Characteristics

3.1. Geomorphological Characteristics of the PTTS Magma System Manifestations

The problems of PTTS genesis were solved based on the analysis of satellite images and geological maps. The PTTS manifestation areas, the geology of which is illustrated in Figure 1, demonstrate the coincidence of morphological structures of the WSP basement overlapped by sedimentary rocks with the basement structures in the WSP and Kara Sea petroleum basins (Figure 2) [48- 53]. Morphological structures characteristics of the PTTS volcanic formations do not significantly differ in areas covered by Meso-Cenozoic sediments (Figure 1), which is confirmed by data on the thickness of the sedimentary rocks in the petroleum basin (Figure 3) [48]. The largest volcanoes and volcanic ridges can be revealed, which are also recorded on maps of magnetic [35] and gravitational anomalies. These works [16], evidencing the development of volcanic processes in the PTTS formation on a single tectonic platform basement, suggest that during the development of Mesozoic downfolds there was mainly an increase in the distances between volcanic edifices without the formation of large faults, as recorded in the Tunguska syncline. These assumptions should be confirmed by the presence in regional maps of the corresponding morphology and distributions of magnetic and gravitational anomalies, which provide rift isolation [8,20,54-55].

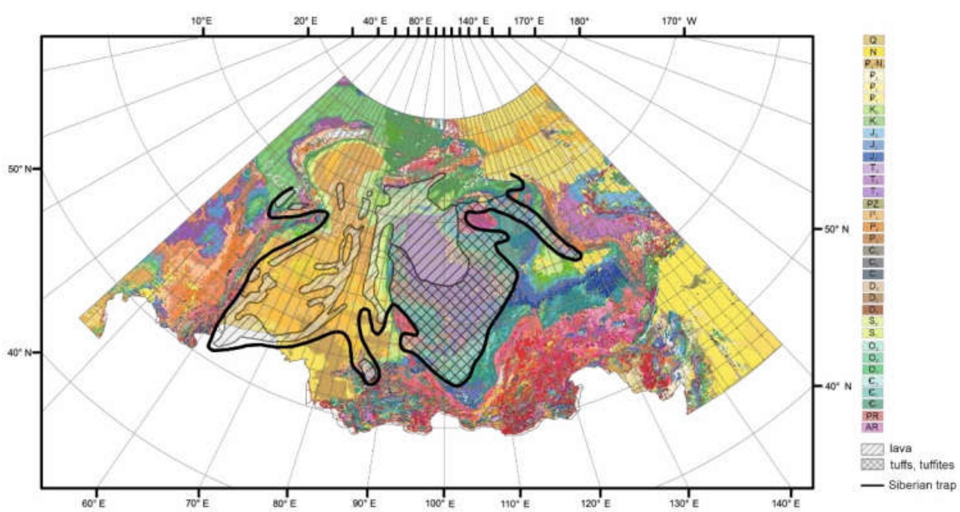

Figure 1. Fragment of the State Geological Map of Russia for the manifestation region of the Permo-Triassic formation of Siberian traps (see the contour boundaries) and adjacent territories. Purple color indicates the contours of the field of igneous PTTS of Tunguska syncline.

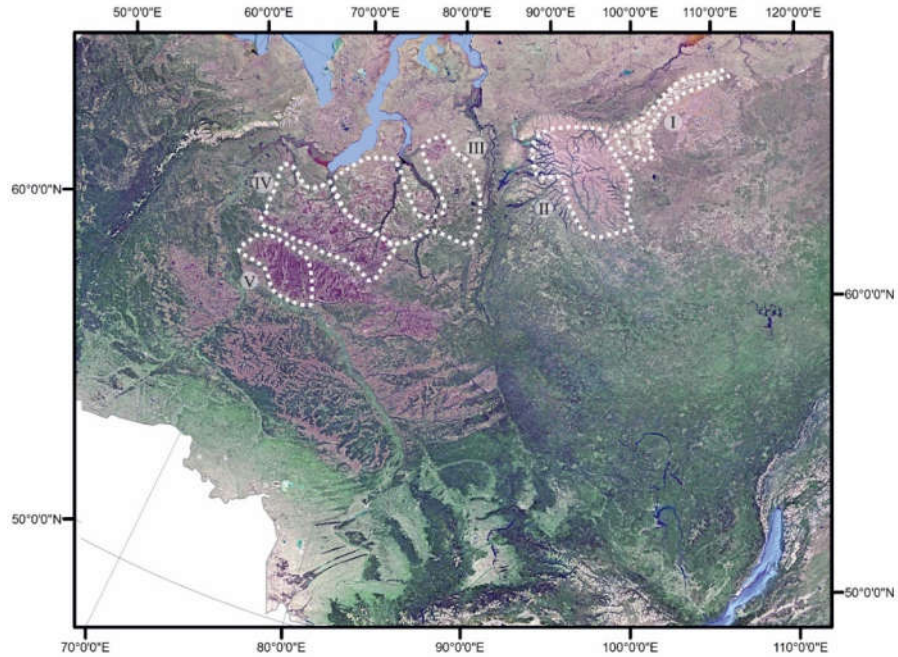

Figure 2. The PTTS areas with igneous trap manifestations and intrusive bodies on the Earth's surface and under sedimentary rocks of the Meso-Cenozoic cover of the Siberian Craton, Taimyr and West Siberian Plate (see Figure 1) (I) northwestern volcanic zone of the Anabar shield (with manifestations of stratovolcanoes), (II) western and central parts of the Tunguska syncline, (III, IV) central and northwestern volcanic zone of the West Siberian plate, (V) junction area of volcanic structures of the Urals and West Siberian Plate.

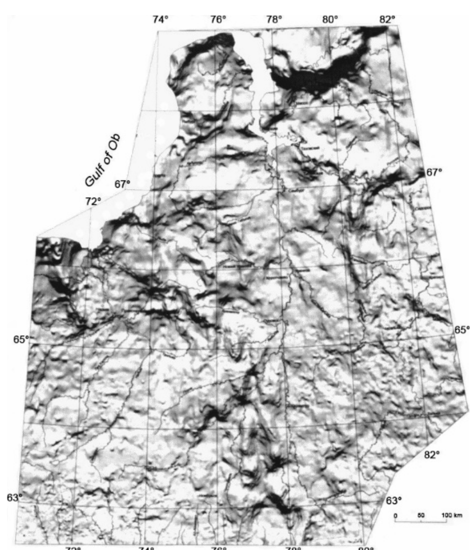

Figure 3. Surface map of the petroleum basin basement of the West Siberian Plate [48].

3.2. Comparison of Location and Morphology of the WSP Intrusive Bodies and Volcanic Edifices

Systems of regional latitudinal, meridional and intermediate lineaments controlling the location of igneous bodies on the SC territory were recognized in [34,36]. In the southern SC, a similar local distribution of igneous rocks, dike belts and pipe-shaped ores was

Preprints (www.preprints.org) | NOT PEER-REVIEWED | Posted: 2 March 2022 doi:10.20944/preprints202203.0045.v1

shown in [22,24,56,57]. The uncertain structural interpretation of geophysical maps may be related to the presence of extended sub-volcanic sills [27,58] and lava covers above dikes [28], as well as with the pre/post trap discontinuities and earlier manifestations of magmatism in the earth's crust [59-62]. Only the regional pattern of the distribution and morphology of magma-permeable zones in the crust is discussed below. It is worth mentioning that the magma rock bodies of different ages cannot be separated using these techniques. This is characteristic of WSP, in which part of the PTTS manifestation region under Mesozoic sedimentary strata is overlapped by the development area of Middle Paleozoic volcanic complexes [63].

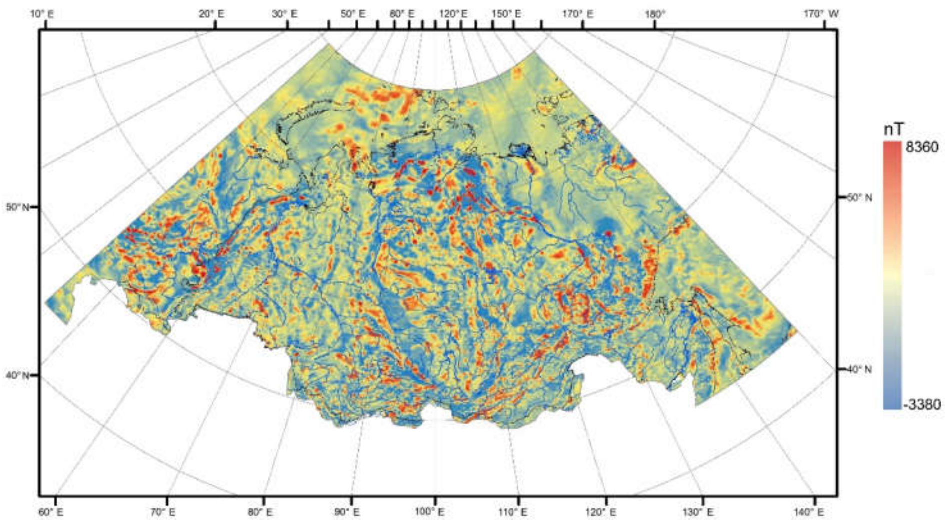

Figure 4. Map of lithospheric magnetic anomalies for the manifestation areas of the Permo-Triassic traps of Siberia (model EMAG2 v.3, [70]).

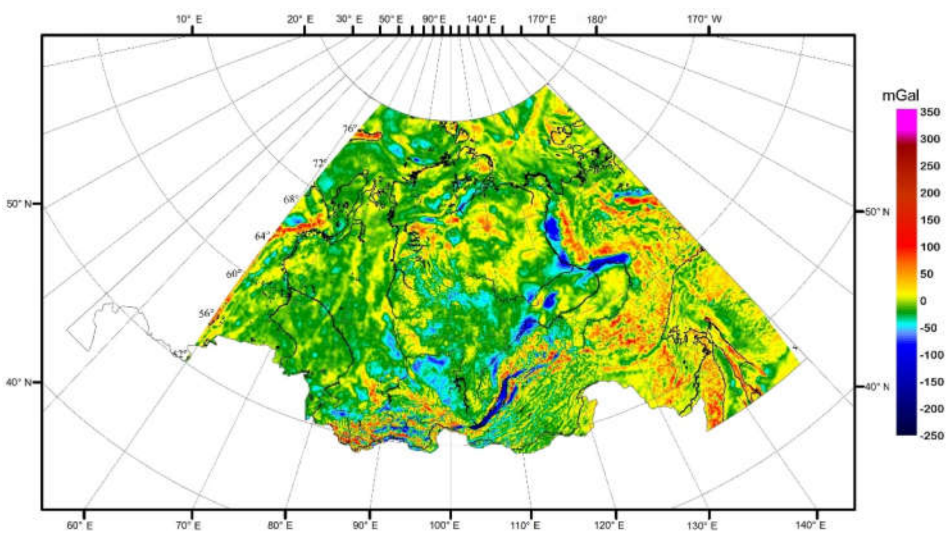

Figure 5. Map of gravity anomalies in free air for the PTTS area (model DTU15 [71]).

The study of the problem based on the analysis of magnetic and gravitational anomalies enhances the accuracy of structural interpretations. Maps of the boreal segment of the Earth above 60° contain the data [38]. Systems of magnetic and gravitational anomalies and individual causative objects can be compared with the objects in Figures 2 and 3 to identify the PTTS manifestation regions and the largest lineaments interpreted as fault zones, which control the manifestations of basic intraplate magmatism [7,8,55,63] in the northern PTTS. A comparison shows the correspondence of position and dimensions of magma formations to magnetic and gravitational anomalies (Figures 4 and 5). Correlation with the relief of the basic horizons of Mesozoic sediments in petroleum basins [17,48-51,53] demonstrates the consistency of the main morphological structural elements of the crystalline basement of petroleum basins on the PTTS manifestation territory and morphological characteristics of magnetic and gravitational anomalies.

3.3. Structural Characteristics of the PTTS Volcanic Manifestations

Articles on the PTTS geology and development are devoted mainly to the nature of ore-bearing intrusive rocks and magma rock sections of volcanic synclinal folds of the SC northwestern, northern, southern and southeastern parts [21,26,58]. The geological map of Russia reflects an objective geological pattern of the manifestation of PTTS volcano-plutonic complexes (Figure 1). The structural characteristics of PTTS in the pattern of igneous complexes of different ages in the boreal and middle-latitude region of the Earth can be obtained from the comparison of the tectonic map [55] and tectonics of the boreal region [64] with magnetic maps (Figure 4) and gravitational (Figure 5) anomalies above 60° north latitude and with maps of volcano-plutonic complexes [63], as well as with data from the works [3,34-35]. To compare these data with the characteristics of the PTTS development area, an analysis of the magnetic anomaly map for this area was made. Figure 4 supplemented the data [34,36] shows the morphology and distribution of magnetic-causative bodies interpreted as volcanic and volcano-plutonic rocks on the WSP, Taimyr and SC territory covered by a sedimentary cover and as volcanic and plutonic mafic rocks on the SC areas. Data correlation in Figures 2 and 3 shows a good agreement of the forms and places of localization of volcanic rocks on the WSP area, Kara basin and Khatanga trough and the crustal morphological structures reported in [17,49-51,53,65]. Correlation with local gravitational anomalies for the PTTS manifestation area (Figure 5) shows the consistency of the main structural elements reflecting the position and configurations of morphological structures: the overlapping of the morphology of large volcanic ridges with band magnetic and gravitational anomalies; morphology of individual development sites of magma rocks is fixed for all scales.

An important factor for understanding the nature of the magmatic phenomenon of the lithosphere in the northern Asian continent is the heterogeneity of intensity and morphology of the volcanism manifestation, which is correlated with the Anabar craton (I) (Figure 1): occupied from the west of this contour by Tunguska syncline (II) with the maximum scales of volcanism; configuration of the eastern PTTS, in which its alignment with the Lena aulacogen structures is recorded [63, 66-67]. Four sectors can be distinguished, different in morphological structures and intensity of the PTTS igneous systems development, concerning Anabar craton. The northern sector of the PTTS manifestation in Taimyr is divided by the "Rosen lineament" [61,68] into two subregions and can be traced along the east boundary of the Tunguska syncline to the south SC boundary. The western sector consists of three subregions - the Tunguska syncline, the latitudinal band of the Yenisei shear zones [69], and mainly meridional WSP faults. The southern (Angara) sector is divided by a meridional fault into western and eastern subregions. Its geology and structural features have been described in detail in publications on the study of ore and petroleum fields. The eastern (Vilyui) sector at the interface with the southern sector has been well studied in [28] for its western part, and in [63, 66-67] for other parts. Its characteristics can be seen from the analysis of lithospheric magnetic anomalies presented in Figure 4 (model EMAG2 v.3, [70]) and gravitational anomalies in free air given in Figure 5 (model DTU15 [71]). The tectonophysical position of the Novaya Zemlya-Kara sector and its joints with the structures of the Ural belt, as well as the nature of the northern PTTS boundaries and the Mesozoic basic igneous systems of Taimyr, is vague concerning the traps manifestation outside the contour depicted on the geological map (Figure 1). Geodynamic analysis of the terrain composition nature of the earth's crust development in the PTTS manifestation region was made in [7,8,55,64,72]. The spatial characteristics of the junction in regions of the Mesozoic tectonic-magmatic cycle of igneous systems development of the boreal area of the Earth and East Siberia with the PTTS manifestation site require further study. Mesozoic and Cenozoic non-volcanic sedimentary basins with their own tectonics have developed on this territory [37,49-51], the formation of which may be included in the history of rift structures [8,73].

3.4. Structural Characteristics of Magmatic Systems of the Taimyr and SC Trap Formation

The Taimyr traps, Khatanga trough and their junction with synclinal folds calderas of the northern SC are poorly described due to the presence of a cover of Mesozoic and Cenozoic deposits [29]. It should be noted that the geological map of Taimyr illustrates two strips of traps parallel to the metamorphic rocks belt, with their shifts along with the system of northwestern faults. Given the significant overlap of Taimyr with sedimentary rocks, it can be assumed that such an interpretation does not explain the "volcanic belts" structure of Permo-Triassic traps. Based on the analysis of maps of magnetic and gravitational anomalies (Figures 4 and 5) we propose another interpretation of the structural characteristics of volcanic systems in the northern PTTS development area. Figures 6 and 7 reflect a more detailed pattern of the structure of this trap volcanism sector. Taking into account the data in [17,51,53], we suggest the presence of a specific area under the Mesozoic and Quaternary deposits of PTTS igneous structures, which is a northern continuation of SC synclinal folds [29].

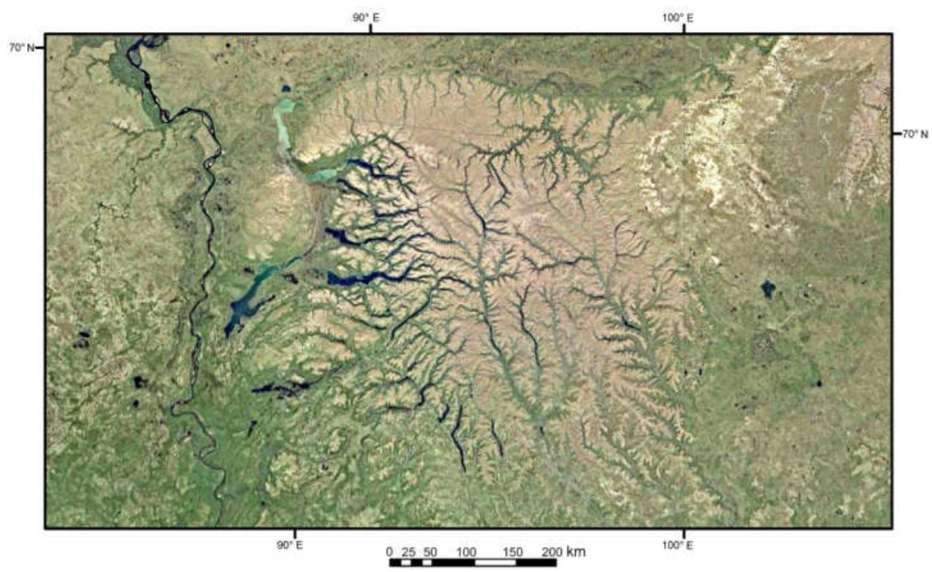

Figure 6. The PTTS area of the Khatanga trough in Siberian Craton and adjacent areas of Taimyr and Siberian Craton: morphology of volcanic edifices, depressions and bottoms of the ridges are filled with the earlier igneous rocks.

The volcanic morphological structures of the Khatanga trough in the Taimyr and SC junction are shown in Figure 6. A similar pattern was obtained for local gravitational anomalies by GIS-ENDDB (Figure 7). It is assumed that the SC area detected by local anomalies in its basement subsidence along the faults along the latitudinal fault, caused by the asymmetric meridional stretching of the crust, covered the northern Tunguska syncline. Figure 6 presents a zone affected by the stretching in PTTS igneous systems by an intersection point of volcanic ridges in the junction of the arcuate fault of the Khatanga trough and stretching area of the Tunguska syncline crust. The northern PTTS sector reflects the continuation of this structure in the platform cover of Taimyr, where the meridional component of stress dominated during the PTTS formation. The northern boundary of this PTTS part is not distinguished, since the tectonic sketch maps do not indicate the

Preprints (www.preprints.org) | NOT PEER-REVIEWED | Posted: 2 March 2022 doi:10.20944/preprints202203.0045.v1

field contours of Mesozoic igneous systems and do not demonstrate the fault systems controlling them. The map of gravitational anomalies (Figure 7) reflects postmagmatic tectonics. The development of PTTS igneous systems in the marginal zones of the crust blocks results in their shifting and possible rotating [74]. The latter leads to ring-type and arc volcanic ridges in the northern PTTS and Khatanga stretching zone (Figures 6 and 7) [75]. P.M. Bondarenko experimentally investigated characteristics morphological structures of such zones on optically active media [76].

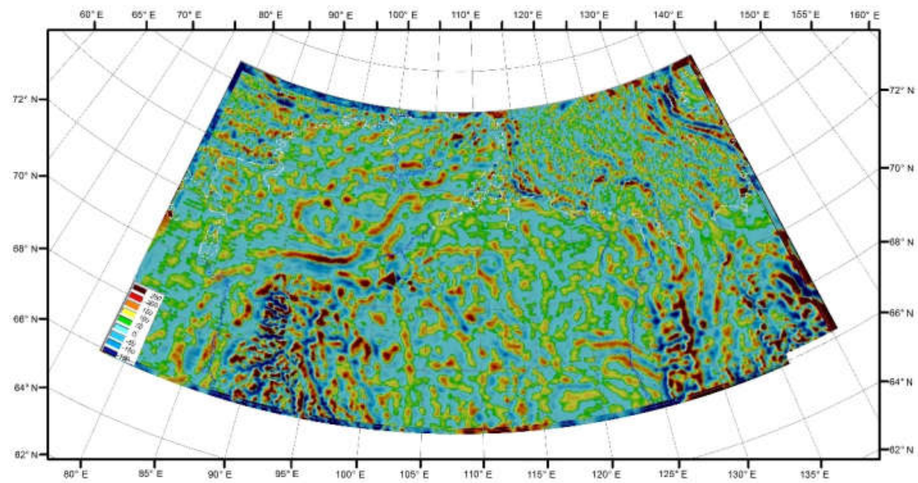

Figure 7. Map of local gravity anomalies (R = 40 km) for Taimyr, Khatanga trough and northern Siberian Craton (based on remote probe data [46] in the form of the shadow model GIS-ENDDB [43]).

Let us consider the structure of PTTS manifestation, according to the analysis of geophysical anomalies and relief features. Along the Anabar craton perimeter (Figures 2 and 6), zoning and significant heterogeneity of the manifestation scales of PTTS volcano-plutonic complexes are observed: the presence of a chain dike belt; a northern and northwestern segment of volcanic ridges with maximum heights of volcanoes; western segment with a minimum thickness of lava flows; southeastern sector with low-thickness mantle flows [28]. The characteristics of the eastern segment were reported in [28,63,66,73]. The southern SC is characterized by the same combination of permeable zones as for the Tunguska syncline, but the scale of mafic melts intrusion is much lower [22,28,56,58]. There is no platform cover on the West Siberian Plate, which led to the predominance of the linear volcanic chain [48](Figure 3) and no stratum-like subvolcanic penetration rocks, which were covered by mantle flows characteristic of SC and Taimyr. The relief analysis (Figures. 2 and 6) allows to compare these results with the data [17,48-51,53,65] and to clarify the position of fault-magma reservoirs in the northern WSP crust, SC platform cover and Taimyr in their junction area [29].

The data provided updated information of the earth's crust structure in the study area reported in [69]. The problem remains on the systems of fault-magma reservoirs in the assumed rifts beneath the WSP sedimentary strata and in the threefold juncture of the Yenisei-Khatanga trough and Ob rift [55]. Correlation of local gravitational and magnetic anomalies with changes in the thickness of the top of Jurassic and the bottom of Mesozoic sediments [48,65] allowed us to conclude that this surface is the bottom of the sedimentary rocks, reflecting the morphology of large volcanic edifices and vents between them. At the same time, two parallel latitudinal depressions of the Khatanga trough formed along with the uplift [65], which has the S-shaped development strip of traps (Figure 7). The geological and structural pattern of sedimentary basins of latitudinal extension to the west of this structure is described in detail in [51,53,77]. This area is assumed as the geodynamic plate juncture according to [55]. The review [78] studies seven variants of threefold plate juncture, according to which the region should contain large tectonic deformations in the crystalline basement and angular deviations of the intended plates boundaries. The second structural and magmatic variant is a similar threefold juncture of volcanic ridges in the axial parts of rift valleys. This juncture of rifts refers to the sections of sedimentary basins reported in the above-mentioned works. Such hypothesis suggests the structural features of the discontinuities junction in the platform cover basement and its crystalline basement of Taimyr - SC, Kara plate and WSP, earth's crust on the SC-WSP boundary, as well as the structure of igneous rock systems in the latitudinal band between the Kharaelakh synclinal folds and the traps of the northern Ural belt (Figures 6 and 7). On the tectonic plot of the platform basement (Figures 4 and 5), there are no signs of a threefold plate juncture and no morphological structure corresponding to the Khatanga rift is present [78-79].

Mesozoic Yenisei-Khatanga trough [50,65] is a post-trap depression of the Kara sedimentary basin, which has its complex subsidence dynamics [50-49,53]. The dynamics of the depression development in connection with the Mesozoic tectonics of petroliferous basins subsidence and Cenozoic drifts of the crust has been studied in [8,73]. In the PTTS study area, the structure of the crystalline basement on which igneous formations develop and magma feeding chambers were recorded on maps of magnetic and gravitational anomalies (Figures 4, 5, 7), as well as on structural maps of the earth's crust and lithospheric mantle [3]. According to Fig. 4 and 5, the structures of the Earth's crust basement on the boundary of WSP and SC are extended north of the assumed juncture and there is no supposed Khatanga rift in the form of an intraplate regional and isolated volcanic zone (Figures 6 and 7). Another development of arc volcanic groups along the latitudinal regional fault is fixed here. The junction of the volcanic zones of Taimyr and similar structures on the WSP and SC boundary is recorded in the western Taimyr (Figures 4 and 5).

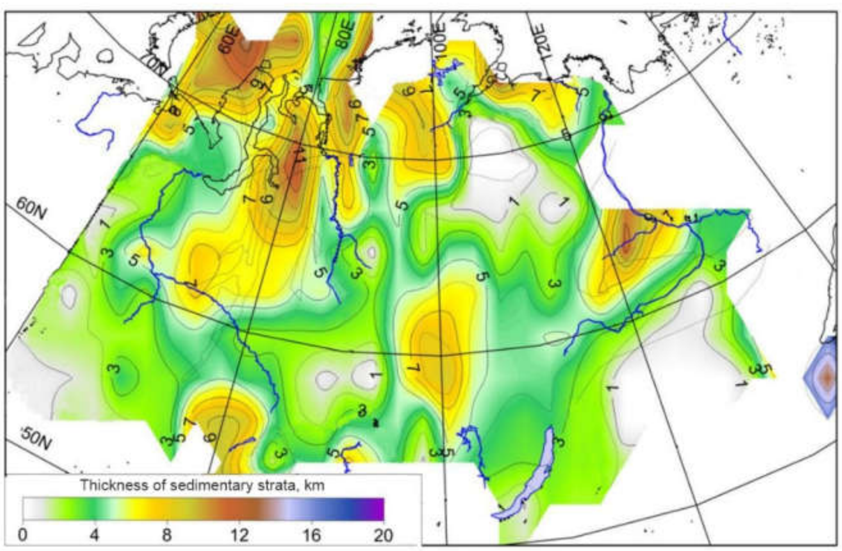

Figure 8. Map of gravity anomalies in free air for the PTTS area (model DTU15 [71]).

Volcanic synclinal folds of the northwestern and northern SC [29] and similar formations of the southern Taimyr form an independent area of magmatism, which intersects with that of the Kara basin (Figures 6 and 7), and likely have a northern continuation. However, its eastern boundary is the meridional fault zone dividing the eastern Taimyr and Anabar shield. There exists a specific Maymecha-Kotui petrochemical province, characteristics of which have no counterparts within the PTTS manifestation. The latitudinal section of the suggested rifting is therefore not observed in the crystalline basement structure on the WSP and SC boundary to the central Taimyr. The Khatanga trough has no linear latitudinal area of stretching and the asymmetric eastern boundary of the Paleozoic

Preprints (www.preprints.org) | NOT PEER-REVIEWED | Posted: 2 March 2022 doi:10.20944/preprints202203.0045.v1

cover subsidence in its bent to south. From the latitudinal fault to the south, an arc of the crust subsidence is presently broken in the Khatanga trough by meridional faults into four sectors. In [65] was reported the formation history of Mesozoic sedimentary belts of the Khatanga trough and their deformation by subsequent tectonic processes. In [8,20,54,73] these phenomena were considered as intraplate rifting.

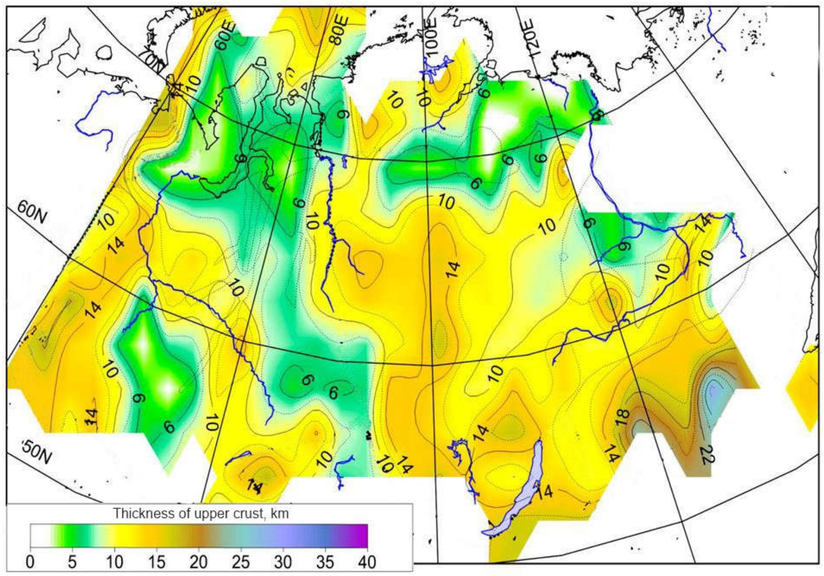

Figure 9. Map of gravity anomalies in free air for the PTTS area (model DTU15 [71]).

For Mesozoic rifting within the WSP [54], it is important to separate rift morphological structures and aulacogens. According to [17, 49-51] there is no need to distinguish classical rift valleys and mid-ocean ridges on WSP the territory. Chains of volcanic edifices covered by Mesozoic sediments are highlighted on the basic horizons of the Mesozoic sedimentary cover. The top of the Cenozoic-Mesozoic deposits reflects the relief of subvolcanic Permo-Triassic volcanism [48]. The morphology and dimensions of magma formations (Figure 3) are consistent with the dimensions of both shield and stratovolcanoes of intraplate volcanic chains [12,80]. It should be taken into account that at the initial stage of trap volcanism the thickness of the Ivakinskaya suite, which formed igneous rocks in eastern Taimyr, was significantly higher than that of the Kharaelakh synclinal folds [29]. The maximum tension field during the development of the magma systems of the Permo-Triassic traps of Taimyr and SC was therefore located in the north direction of the Mesozoic Khatanga trough axis. The formation of sedimentary basins and their following deformations may be associated with the Mesozoic and Quaternary tectonics of the studied plates [51]. Between the SC and Taimyr during the development of igneous PTTS systems, as well as throughout the SC territory there could be no manifestations of classical rifts. This is also evidenced by an isopach map of the upper Earth’s crust (Figures 8 and 9), in which the study area does not have latitudinal boundaries between plates [3]. The nature of morphology of volcanic edifices in the latitudinal strip between the Kara basin, structures of Taimyr, SC and WSP is presented in [48,49,51,60]. Qualitative analysis of the formation dynamics of post-volcanic structures can be carried out according to [49,51].

4. Discussion

Analysis of the morphological structures of the earth's crust in the PTTS development area suggests the presence of deformations in the form of different scale diffused spreading, the local characteristics of which depend on whether there is (SC) or no (WSP) platform cover. The regional distribution of deformations of the lithospheric plate is associated with latitudinal and meridional stretches of the crust and the movement of the SC

Preprints (www.preprints.org) | NOT PEER-REVIEWED | Posted: 2 March 2022 doi:10.20944/preprints202203.0045.v1

largest blocks relative to the craton of the Anabar shield [34,36,75]. Local shifts of the blocks during the formation of the trough are associated with the diffused spreading of the western SC (Tunguska syncline) and the area between the SC and Taimyr (Figures 6 and 7). This igneous rocks region in the west and east coincides with faults and minor volcanic chains; in the southern SC, an area of volcanic edifices and dike belts was formed; within the WSP, a more common system of magma permeable northeastern and northwestern faults is observed. [48]. No classical rift signs were recorded in the PTTS area as confirmed by geophysical maps of the earth's crust structure (Figures 8 and 9).

The PTTS development on the SC territory includes a minimum of two magmatic stages with uncertain spatial manifestations [30]. The location areas of upper igneous and dike rocks can be distinguished (Figures 2 and 6). However, there is no dating of these events and no data exist on the boundaries of petrochemical provinces and the comparison of the WSP and SC magma rocks. For SC, in the direction of decreasing the intensity of magma flow from north to south, the Parana petrochemical trend exhibits an increase in the silica content of basic melts in the lithospheric mantle [81]. Statistical evaluations of the petrochemical compositions of the Siberian traps (Figure 10) show significant spatial differences in their compositions. In WSP, unlike SC, effusive rocks have undergone significant hydrothermal alteration; the general meridional trend of increase in SiO_2 contents is recorded; in the southern SC, the subvolcanic bodies of ore-bearing pipes are enriched with MgO; in the area of trap formation, the average contents of Al, Ti, Si are similar; traps of the Maymecha-Kotui province sharply differ in the contents inclusions and several petrochemical elements from the igneous and intrusive rocks of other SC provinces; the most characteristic is wide variations in the composition of dikes of the Kamenskaya province in the northern margin of the Tunguska syncline. On the WSP, other spatial petrochemical characteristics of magma rocks are recognized [30-33], where the Parana type of volcanism may have been occurred characterized by abundant felsic melts of the final stages of magmatism.

Given the general picture of magmatism, the following features of PTTS generation can be noted: development on the most igneous systems of the statistically pronounced tholeiite mantle melts [21,82]; the presence of melts, which sharply differ in composition from melts of tholeiitic type, in giant faults, in which a wide range of mantle and crustal magmas is fixed. Meridional and northeastern lineaments are present, in which the processes of basic, alkaline and carbonatite magmatism are observed in a wide time span [40,61,68]. These phenomena are expressed in the structure of abnormal zones in the upper mantle.

Tomographic data of strip and vertical sections of the lithospheric and upper mantle are given in Figures 11 and 12. Fields of shear wave velocities with vertical polarization S_v are represented relative to the base velocity S_{vo} according to [83]. Analysis of the structure of lithospheric and upper mantle on tomographic sections beneath the transects - Craton, Meteorite, and Rift [84-85] reveals the presence of plate-shaped areas of an abnormally dense mantle at the depths of 100-240 km. For the diamond-bearing province of the Siberian Craton, sections of mineral facies of compositions of the assumed terranes in the upper mantle were drawn [86]. Maps of the crustal morphological structures compiled in [3] have been supplemented by maps of the lithospheric plate and upper mantle morphological structures for the entire PTTS region. Tomographic maps of transverse waves with vertical polarization were compiled in a depth interval of 50-700 km with an interval of 25 km in depth (Figure 11) using the GIS-ENDDB software [43-44] based on the method [45]. These data update the conclusions that there are no signs of the Khatanga-Ob threefold rift juncture between the slab lithospheric blocks of the WSP, SC and Kara sedimentary basin (Figure 11a); the existence of a single mantle field of PTTS volcano-plutonic magmatism (Figure 11b-d); the existence of diamondiferous carbonatite igneous systems, which spatially separated from the fields of the Middle Paleozoic and Permo-Triassic traps (Figure 11, d-e); the isolation of the non-volcanic Mesozoic convection field under the trap formation (Figure 11f-i); on the different nature in igneous systems under different sectors of the PTTS manifestation area (Figure 11g-i).

Preprints (www.preprints.org) | NOT PEER-REVIEWED | Posted: 2 March 2022 doi:10.20944/preprints202203.0045.v1

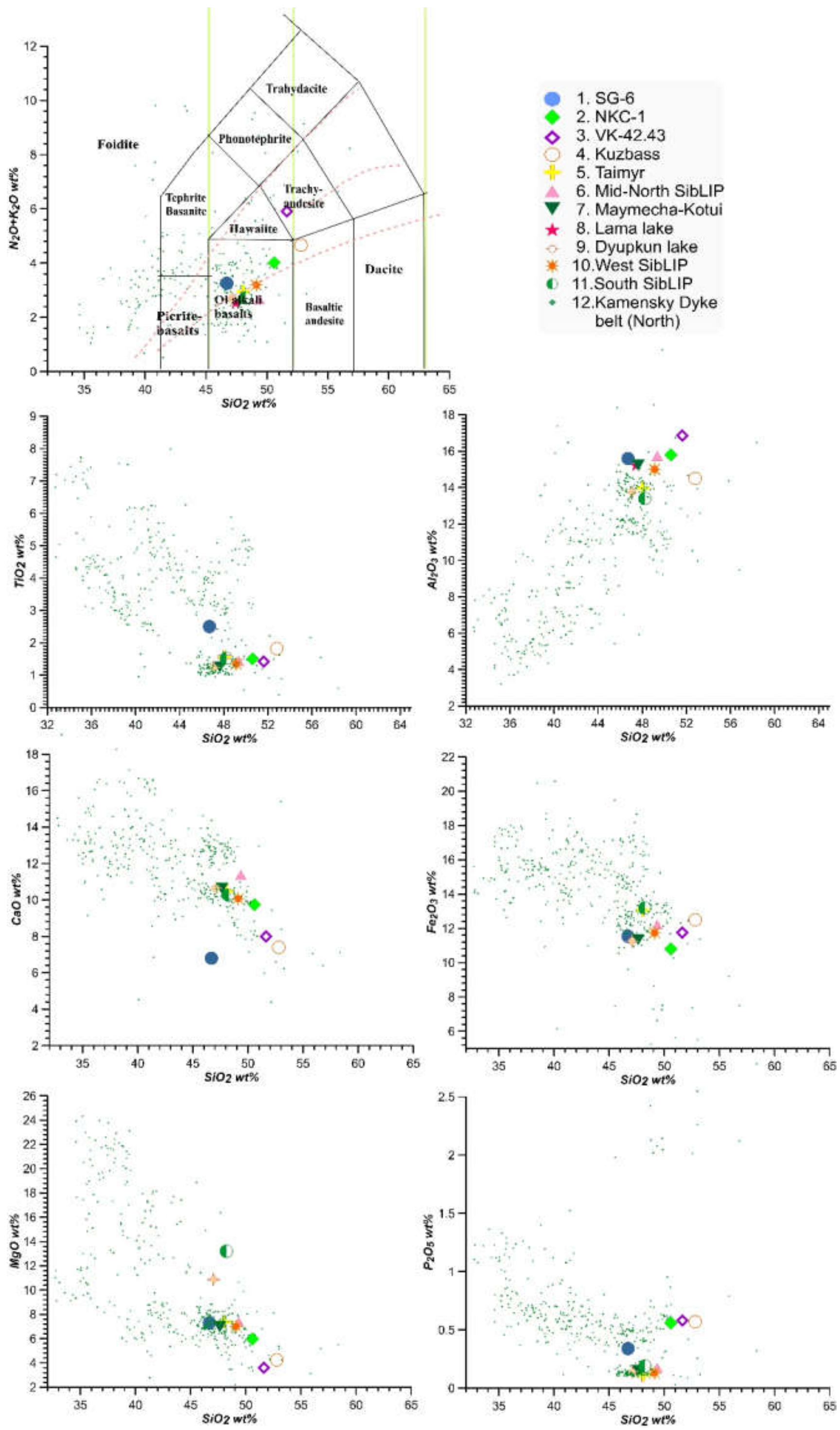

Figure 10. Data of petrochemical compositions in traps from different parts of the West Siberian Plate and the Siberian Craton: (1) SG-6, (2) NKC-1, (3) VK-42.43 - numbers of reference sections in the deep and super-deep wells of the same name [32-33]; (4) Kuzbass [90-91]; (5) Taimyr [92-93]; (6) Mid-North SibLIP - data of Almukhamedov and Medvedev, estimates of Tb/Yb in works [94-95]; (7) Meymecha-Kotui - [96] (for the Onkuchanskaya suite of the Maymecha-Kotui province); (8) Lama lake - authors' data for the volcanic section of its south margin; (9) Dyupkun lake - data for volcanic section of its margins [29]; (10) West SibLIP [92-93]; (11) South SibLIP data by S.D. Kurtseraite, (12) Kamensky Dyke belt (North) - data by [29].

The latter requires the analysis of the heat and mass transfer processes in the convection area of the upper mantle and zones above the asthenosphere of the lithospheric mantle of the crust.

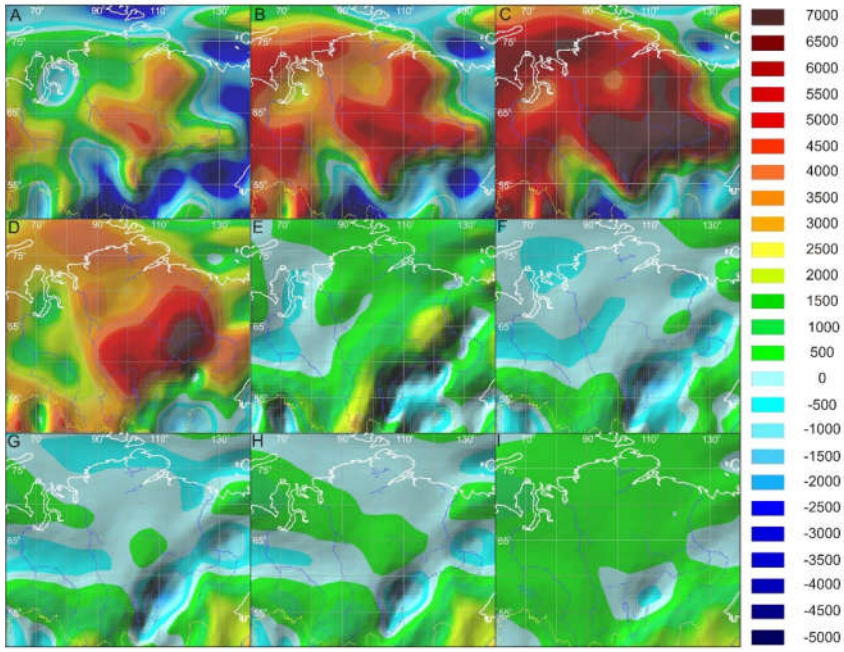

Figure 11. Tomographic maps of S waves anomalies with vertical polarization for the PTTS areas at the depths of 50 (a), 75 (b), 100 (c), 200 (d), 300 (e), 400 (f), 500 (g), 600 (h), 700 (i) km (by data [45] in the form of the shadow GIS-ENDDB model [44], per units (SV-SV0)/SV0*100 %).

A solid slab (Figure11a-c) beneath the PTTS development area can be considered as the melting area of tholeiitic basalts and associated more felsic melts characteristic of the Parana type of traps. High magnesium traps belong to the deeper horizons of the upper mantle. The deepest melting regions of carbonatite fluids released beneath the Siberian Craton (Figure 11 d, e) are located in the northeastern part of the mantle plate under the detected strips of diamondiferous pipes. Characteristics of morphological structures of these magmatic systems have been recorded on tomographic sections (Figure 12).

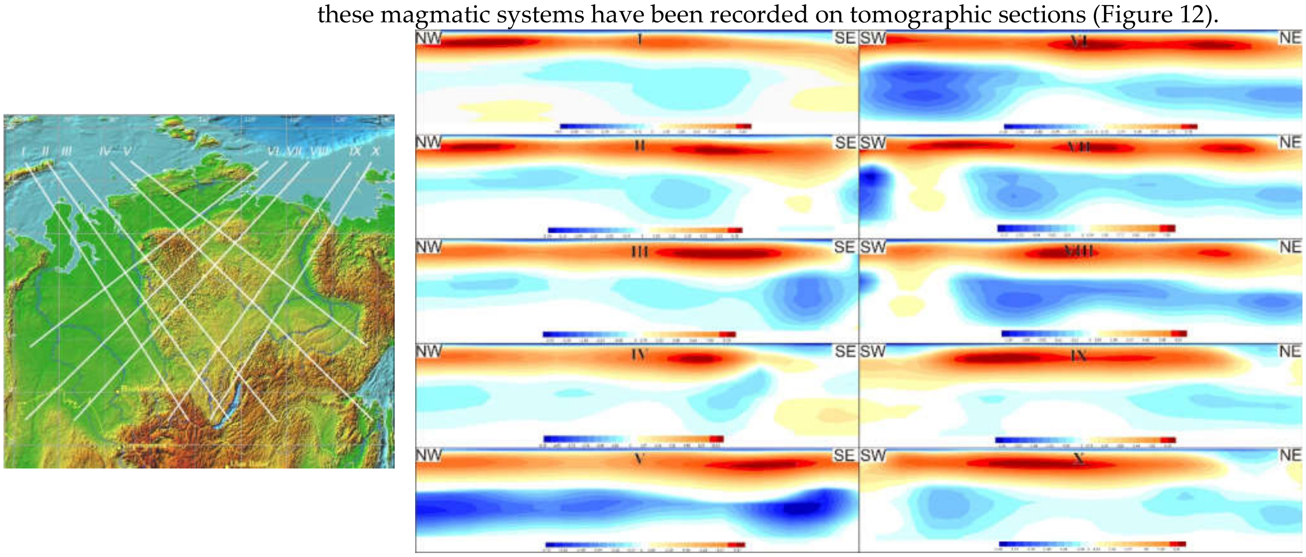

(a) (b)

Figure 12. Schematic diagram of profiles (a) and fields of anomalies of S waves with vertical polarization on vertical sections (b) (50-700 km) according to the presented profiles (according to [45] in the form of sections GIS-ENDDB [44], per units (SV-SV0)/SV0*100 %).

Layered maps of the earth's crust and mantle provide qualitative insights into morphology changes with the depth of sedimentary basins in the crust and convection zones in the upper mantle (Figure 11). In the interpretation of mineral-geochemical data on the composition of mantle xenocrysts and xenoliths in diamond pipes [86], it is important to analyze the change in morphological structures with depth according to the data of vertical sections of the lithosphere and mantle (Figure 12) which cover the area of diamond deposits on the SP [40] and the areas of carbonatite intrusive complexes of all igneous cycles within the Siberian Craton [87]. A feature of the structures presented in Figures 11 and 12 is the isolation of convection zones and heterogeneities in the upper mantle. In the context of the history of PTTS terrestrial volcanism, it can be assumed that the area of PTTS development is a superswell above an abnormally large decompression-melting zone when convection takes place in the upper mantle. This arid climate region [88] did not have large sedimentary basins not only for this reason but served as a total high point of the earth's crust above sea level. This was an additional agent of mainly in subaerial magmatism over extensive areas of the crust stretching. It can be believed that during the crust deformation in the area of PTTS in the subsequent Mesozoic and Cenozoic geodynamic cycles, no visible changes in the position of regional fault zones occurred, but the relief height varied significantly. Models of plume tectonics of LIPs in the development of PTTS igneous systems using the mechanics of inter-block and intra-block deformations of solid media were reported in [74,89].

The formation geodynamics of the trap [3] differs from that of the other trap provinces not only in the absence of a central rift and the opening of the ocean basin [2], but also in the process on the heterogeneous crustal basement of the Asian continent of an extensive volcanic chain in geotectonic fracturing area of the earth's crust. This process is distinct from classical rifting. The general geodynamics of the development of volcanic processes from the middle of Paleozoic in Siberia is reflected in a series of maps [63].

5. Conclusions

Permo-Triassic traps of Siberia were formed along the perimeter of the Anabar craton in the stretching sites of the crust of two continental plates (West Siberian Plate and Siberian Craton), which have a junction at the submeridional boundary. A region of diffused spreading was intensively developed in the western Siberian Craton, in which the Tunguska syncline with a giant volcanic sector formed. In other sectors, the density of fault zones was similar, and the form of magmatism was determined by the presence or absence of a platform cover: volcanic ridge systems developed within the West Siberian Plate; on Taimyr, east and south of the Anabar craton, dike belts, pipes and extended sill intrusions of traps formed. The general elevation of the earth's crust in the northern Asian continent during this period of geological history over the giant area of the anomalous upper mantle has determined the predominance of subaerial volcanism forms. The construction of a physical model of such a special state of the upper mantle [1] requires special study with reference to the above data.

Author Contributions: Conceptualization, V.S.; methodology, V.S. and Y.P.; software, A.M.; investigation, V.S., Y.P., A.M., and A.B.; writing-original draft preparation, V.S. and Y.P.; writing-review and editing, A.M., I.A., and A.B.; visualization, A.M., I.A. and V.L. All authors have read and agreed to the published version of the manuscript.

Funding: The work was done on state assignment of IGM SB RAS and partial financial support of the RFBR grant 19-05-00788.

Data Availability Statement: Not applicable.

 doi:10.20944/preprints202203.0045.v1

Acknowledgments: The authors thank to A.N. Vasilevsky for his help in preparing maps of gravitational and magnetic fields for the boreal region of the Earth. Authors greatly appreciate K.V. Chudnenko, P.S. Lapin, M.P. Mazurov, V.V. Ryabov, A.A. Tomilenko, and A.N. Vasilevsky for critical problem discussions, and M.M. Eletsky for assistance in the technical editing of the manuscript.

Conflicts of Interest: The authors declare no conflict of interest.

References

1. Zonenshain, L.P.; Kuzmin, M.I. *Paleotectonics*; Publishing House Nauka: Moscow, Russia, 1992; 126 p.
2. Courtillot, V.; Jaupart, C.; Manighetti, I.; Tapponnier, P.; Besse, J. On causal links between flood basalts and continental breakup. *Earth Planet. Sci. Lett.* **1999**, *166*, 177–195.
3. Cherepanova, Y.; Artemieva, I.M.; Thybo, H.; Chemia, Z. Crustal structure of the Siberian Craton and the West Siberian basin: An appraisal of existing seismic data. *Tectonophys.* **2013**, *609*, 154–183.
4. Saunders, A.D.; Jones, S.M.; Morgan, L.A.; Pierce, K.L.; Widdowson, M.; Xu, Y.G. Regional uplift associated with continental larger provinces: The role of mantle plumes and lithosphere. *Chem. Geol.* **2007**, *241*, 282–318.
5. McKenzie, D. The generation and compaction of partial molten rock. *J. Petrol*. **1984**, *25*, 713–765.
6. Dobretsov, N.L. Geological consequences of the plume thermochemical model. *Russ. Geol. Geophys*. **2008**, *49*, 587–604.
7. Dobretsov, N.L.; Vernikovsky, V.A.; Karyakin, Y.V.; Korago, E.A.; Simonov, V.A. Mesozoic-Cenozoic volcanism and stages of geodynamic evolution of the Central and Eastern Arctic. *Russ. Geol. Geophys*. **2013**, *54*, 1126–1144.
8. Dobretsov, N.L.; Reverdatto, V.V.; Polyansky, O.P.; Babichev, A.B. Dynamics of petroleum basins in Arctic and adjacent territories as a reflection of mantle plumes and rifting. *Russ. Geol. Geophys*. **2013**, *54*, 1145–1161.
9. Saunders, A.D.; England, R.W.; Reichow, M.K.; White, R.V. A mantle plume origin for the Siberian traps: uplift and extension in the West Siberian Basin, Russia. *Lithos* **2005**, *79*, 407–424.
10. Trubitsyn, V.P.; Bobrov, A.M.; Kubyshkin, V.V. The influence of the continental lithosphere on the structure of mantle thermal convection. *Izvest. Phys. Solid Earth* **1993**, *5*, 3–11.
11. Bobrov, A.M.; Trubitsyn, V.P. Evolution of viscous stresses in the mantle and in drifting continents during the formation and decay of the supercontinent. *Izvest. Phys. Solid Earth*. **2003**, *12*, 3–13.
12. Sharapov, V.N.; Akimtsev, V.A.; Dorovsky, V.N.; Perepechko, Y.V.; Cherepanov, A.N. *Dynamics of the Development of Ore-Magmatic Systems of Spreading Zones*; Publishing House SB RAS: Novosibirsk, Russia, 2000; 404 p.
13. Sharapov, V.N.; Mazurov, M.P.; Perepechko, Yu.V. Model analysis of trap mantle-crust and ore-igneous systems of the Siberian Craton. *Russ. Geol. Geophys.* **2008**, **49**, 1205–1226.
14. Sharapov, V.N.; Perepechko, Yu.V.; Perepechko, L.N.; Rakhmenkulova, I.F. The nature of mantle sources of Permian-Triassic traps of the West Siberian Plate and Siberian Craton. *Russ. Geol. Geophys*. **2008**, *49*, 652-663.
15. Sharapov, V.N.; Perepechko, Y.V.; Sorokin, K.E.; Kuznetsov, G.V. On the problem of determining the depth of formation and composition of the mafic melt in the upper mantle. *Russ. Geol. Geophys*. **2013**, *54*, 390–409.
16. Farnetani, C.C.; Hofmann, A.W. Dynamics and internal structure of a lower mantle plume conduit. *Earth Planet. Sci. Lett.* **2009**, *282*, 314–322.
17. Kontorovich, V.A. Structure and petroleum content of the western part of the Yenisei-Khatanga regional trough. *Russ. Geol. Geophys.* **2011**, *52*, 1027–1050.
18. Surkov, V.S.; Jero, O.G. *Basement and the Development of the Platform Cover of the West Siberian Plate*; Publishing House Nedra: Moscow, Russia, 1981; 143 p.
19. *Tectonic Map of the Petroleum-Bearing Provinces of the Siberian Craton (1:2,500,000)*; Rovnin, L.I., Semenovich, V.V., Trofimuk, A.A., Eds.; Publishing House SNIIGGiMS: Novosibirsk, Russia, 1982.
20. Grinev, O.G. Rift Systems of Siberia: Methodology for the Study, Morphotectonics, Minerageny; STT Publishing: Tomsk, Russia; 2007, 434 p.
21. Zolotukhin, V.V.; Vilensky, A.M.; Dyuzhikov, O.A. *Siberian Craton Basalts*; Nauka Publishing: Novosibirsk, Russia; 1986, 246 p.
22. Pukhnarevich, M.M. Conditions and Features of the Formation of Endogenous Iron Deposits in the Southern Siberian Craton; Publishing House of Irkutsk University: Irkutsk, Russia, 1986; 336 p.
23. *The Taimyr Subsoil*; Malich, N.S., Ed.; Publishing House B.C.: St. Petersburg, Russia, 1999; 235 p.
24. Fon der Flaas, G.S.; Nikulin, V.I. *Atlas of Structures of Ore Fields of Iron Ore Deposits*; Publishing House of Irkutsk University: Irkutsk, Russia, 2000; 192 p.
25. Nikulin, V.I.; Lelyukh, M.I.; Fon der Flaas, G.S. *Diamond Forecast*; Publishing House ALROSA: Irkutsk, Russia, 2001; 311 p.
26. Dodin, D.A. *Metallogeny of the Taimyr-Norilsk Region*; Nauka Publishing: St. Petersburg, Russia, 2002; 717 p.
27. Prusskaya, S.N. Petrology and the Structural Position of the Intrusive Traps of the West Siberian Platform; Publishing House SFU: Krasnoyarsk, Russia, 2008; 247 p.
28. Korobkov, I.G.; Evstratov, A.A.; Milshtein, E.D. *Basic Volcanic Structures of Diamond-Bearing Areas of the Eastern Tunguska Syncline Margin*; Publishing House STT: Tomsk, Russia, 2013; 270 p.
29. Ryabov, V.V.; Shevko, A.Y.; Gora, M.P. Magmatism and Ore Formation in the Siberian Norilsk Region. Modern Approach in Solid Earth Sciences; Springer: Dordrecht, Heidelberg, 2014; Volume 1, 300 p.
30. Ivanov, K.S.; Koroteev, V.A.; Pecherkin, M.F.; Fedorov, Y.N.; Erokhin, Y.V. History of geological development and basement structure of the western West Siberian petroleum megabasin. *Russ. Geol. Geophys*. **2009**, *50*, 484–501.
31. Medvedev, A.Y.; Almukhamedov, A.I.; Kirda, N.P. Geochemistry of Permo-Triassic volcanites of West Siberia. Russ. *Geol. Geophys*. **2003**, *44*, 86–100.

32. Saraev, S.V.; Baturina, T.A.; Ponomarchuk, V.A.; Travin, A.V. Permian-Triassic volcanites of the Koltogorsk-Urengoy rift of the West Siberian geosyncaline. *Russ. Geol. Geophys*. **2009**, *50*, 4–20.
33. Saraev, S.V.; Baturina, T.P.; Travin, A.V. Petrology, sedimentology, geochemistry and absolute age of sedimentary-volcanic deposits of the Triassic in the southwestern West Siberian geosyncline (Kurgan region). *Russ. Geol. Geophys*. **2011**, *52*, 1107–1128.
34. Witte, L.V.; Vasilevsky, A.N.; Pavlov, E.V. Regional magnetic and gravitational anomalies of the Siberian Craton and their geological nature. *Geophys. J*. **2009**, *31*, 21–40.
35. Braitenberg, C. New insights into the basement structure of the West Siberian Basin from forward and inverse modeling of GRACE satellite gravity data. *J. Geophys. Res*., **2009**, *114 B6*, 1 – 15.
36. Witte, L.V.; Vasilevsky, A.N. Geological nature of the regional magnetic and gravitational anomalies of the Mongolian-Asian province of the Central Asian folding belt. *Russ. Geol. Geophys*. **2013**, *54*, 1851–1860.
37. Surkov, V.S.; Kuznetsov, V.A.; Staroseltsev, V.S.; Salnikov, A.S. Seismic tomography in studying the earth's crust of Siberia. *Reg. Geol. Metallog.* **2000**, *10*, 117–124.
38. Kulakov, I.Y.; Gayna, K.; Dobretsov, L.N.; Vasilevsky, A.N.; Bushenkova, N.A. Reconstruction of plate movement in the Arctic region based on a comprehensive analysis of gravitational, magnetic and seismic anomalies. *Russ. Geol. Geophys*. **2013**, *54*, 1198–1125.
39. Rasskazov, S.V.; Brandt, S.B.; Brandt, I.S.; Ivanov, A.V. *Radioisotope Geology in Problems and Examples*. Geo Publishing House: Novosibirsk, Russia, 2005; 150 p.
40. Pokhilenko, N.P.; Afanasyev, V.P.; Sobolev, N.V.; Egorov, K.N.; Smelov, A.P.; Kostrovitsky, S.I. Stages of kimberlite magmatism of the Siberian Craton and their productivity: patterns of formation and features of forecasting of indigenous diamond deposits of various genetic types, new promising regions. In *Problems of Mineralogy of Russia*; Rundqvist, D.V., Bortnikov, N.S., Safonov, Y.G., Eds.; Publishing House of the Russian Academy of Sciences: Moscow, Russia, 2012; p. 265–285.
41. Mikheeva, A.V.; Dyadkov, P.G.; Marchuk, A.G. Geoinformation system GIS-EEDB and methods of space-time analysis of seismological data. *Geoinformatics* **2013**, *2*, 58-65.
42. Mikheeva, A.V.; Perepechko, Y.V.; Sorokin, K.E.; Sharapov, V.N. Dynamics of convective heat and mass transfer in permeable parts of seismofocal zones of the Kamchatka region and conjugated volcanic arcs. In Proceedings of the XIII International Scientific and Practical Conference New Ideas in the Earth Sciences, Moscow, Russia, 3–5 December 2019.
43. Mikheeva, A.V. Geostructural Elements Identified by Mathematical Algorithms and Digital Models of the GIS-ENDDB Geoinformation and Computing System; Omega Print: Novosibirsk, Russia, 2016; 297 p.
44. Mikheeva, A.V. Expert system GIS-ENDDB and tasks of deep tectonics research. In Proceedings of the XIII International Scientific and Practical Conference New Ideas in the Earth Sciences, Moscow, Russia, 3–5 December 2019.
45. Schaeffer, A.J.; Lebedev, S. Global shear speed structure of the upper mantle and transition zone. *Geophys. J. Int.* **2013**, *194*, 417–449.
46. Sandwell, D.T.; Müller, R.D.; Smith, W.H.F.; Garcia, E.; Francis R. New global marine gravity model from CryoSat-2 and Jason-1 reveals buried tectonic structure. *Science*, **2014**, *346*, 65-67.
47. Pavlis, N.K.; Holmes, S.A.; Kenyon, S.C.; Factor, J.K. An Earth Gravitational Model to Degree 2160. In Proceedings of the General Assembly of the European Geosciences Union, Vienna, Austria, 13-18 April 2008.
48. Deev, E.V.; Zinoviev, S.V. Morphotectonics of the top of the lower structural stage of cover of the West Siberian Plate in the Nadym-Taz interfluve. *Oil Gas Geol*. **1999**, *7-8*, 2–9.
49. Kontorovich, V.A.; Belyaev, S.Y., Kontorovich, A.E.; Krasavchikov, V.O.; Suprunenko O.I. Tectonic structure and history of development of the West Siberian geosyncline in the Mesozoic and the Cenozoic. *Russ. Geol. Geophys*. **2001**, *42*, 1832–1845.
50. Kontorovich, A.E.; Burstein, L.M.; Malyshev, N.A.; Safronov, P.I.; Guskov, S.A.; Ershov, S.V.; Kazanenkov, V.A.; Kim, N.S.; Kontorovich, V.A.; Kostyreva, E.A.; Melenevsky, V.N.; Livshits, V.R.; Polyakov, A.A.; Skvortsov, M.B. Historical and geological modeling of oil generation processes in the Mesozoic-Cainozoic sedimentary basin of the Kara Sea (basin modeling). *Russ. Geol. Geophys*. **2013**, *57*, 1179–1226.
51. Kontorovich, V.A.; Ayunova, D.V.; Gubin, I.A.; Yershov, S.V.; Kalinin, A.Y.; Kalinina, L.M.; Kanakov, M.S.; Solovyov, M.V.; Surikova, E.S.; Shestakova, N.I. Seismostratigraphy and history of formation and gas content of Nadym-Pur interfluve structures (West Siberia). *Russ. Geol. Geophys*. **2016**, *57*, 1583–1595.
52. Druzhinin, V.S.; Martyshko, P.S.; Nachapkin, N.I.; Osipov, V.Y. *Structure of the Upper Part of the Lithosphere and Petroleum Content of the Ural Region Earth's Interior*; GI UB RAS Publishing: Ekaterinburg, Russia, 2014; 236 p.
53. Afanasenkov, A.V.; Nikishin, A.I.; Unger, A.V. Mezo-Cenozoic history of the development of North-West and East Siberia based on the analysis of seismic data (Gydan, Ust-Yenisei district). *Oil Gas Geol*. **2017**, *1*, 34–40.
54. Surkov, V.S.; Smirnov, L.V.; Jero, O.G. Early Mesozoic rifting and its influence on the structure of the West Siberian Plate lithosphere. *Russ. Geol. Geophys*. **1987**, *9*, 3-11.
55. Explanatory Note to the Tectonic Map of the Kara and Laptev Seas and the North of Siberia (1:2 500 000); Bogdanov, N.A., Khain, V.E., Eds.; ILOiVM RAS: Moscow, Russia, 1998; 127 p.
56. Varand, E.L. Geology, Trap Magmatism and Metallogeny of the Southern Part of the Lower Yenisei Metallogeny Zone. PhD Thesis, Novosibirsk State University, Novosibirsk, 1974.

57. Sapronov, N.L. *Ancient Volcanic Structures in the Southern Tunguska Syncline*; Publishing House Nauka: Novosibirsk, Russia, 1986; 97 p.
58. Feoktistov, G.D. Petrology and Conditions for the Formation of Dolerite Sills. Doct. thesis, Irkutsk, 1983.
59. Kuzin, I.L.; Eremenko, V.N.; Ignatovskaya, I.N.; Kalinina, I.N.; Pyatnitsky, V.K.; Ferens-Sorovsky, A.A. Cosmotectonic map of the petroleum areas of Siberia and the Timan-Pechora province. *Earth Res. Space* **1990**, *4*, 42–48.
60. Sim, L.A.; Bryantseva, S.V.; Chekmarev, K.A. On the change of the structural plan of the northern West Siberian Plate and polar Urals. In *Problems of tectonophysics*; Rebetsky, Y.L., Ed.; Publishing House of the Schmidt Institute of Physics of the Earth RAS: Moscow, Russia, 2008; pp. 301–318.
61. Bush, V.A. New data on the structure of the Baikal-Taimyr lineament and divided mega-blocks of the basement of the Siberian Craton. In *Modern geophysical methods and technologies*; Babyants, P.S., Bush, V.A., Eds.; LTD Aerogeophysics: Moscow, Russia, 2009; Volume 1, pp. 111–142.
62. Shevchenko, B.F.; Goroshko, M.V.; Didenko, A.N.; Guryanov, V.A.; Staroseltsev, V.S.; Salnikov, A.S. Deep structure, Mesozoic tectonics and geodynamics of juncture area of the eastern Central Asian belt and Siberian Craton. *Russ. Geol. Geophys*. **2011**, *52*, 2122–2131.
63. Atlas of Paleovolcanic Maps of Northeastern Eurasia (Territory of Russia and other CIS Countries). Scale 1: 5 000 000. Explanatory note; Mapping Factory VSEGEI Publishing: Saint-Petersburg, Russia, 2001; 88 p.
64. Lobkovsky, L.I. Geology of deformed lithospheric plates and a model of regional geodynamics in relation to the Arctic and Northeast Asia. *Russ. Geol. Geophys*. **2016**, *57*, 476–495.
65. Fomin, M. A modern structure of the Mesozoic cover of the Yenisei - Khatangsky regional deflection along the reference levels. *Petrol. Geol. Theor. Appl. Stud.* **2010**, *10*, 1-10.
66. Gaiduk, V.V. *Vilyui Middle Paleozoic Rift System*; YA SB USSR AS Publishing: Yakutsk, Russia, 1988; p. 125.
67. Polyansky, O.P.; Prokopyev, A.V.; Koroleva, O.D.; Tomshin, M.D.; Reverdatto, V.V.; Babichev, A.; Sverdlova, V.G.; Vasilyev, D.A. The nature of a thermal source of basic magmatism of the Vilyuichinsky rift based on the dike belts age and numerical modeling. *Russ. Geol. Geophys*. **2018**, *59*, 1519-1541.
68. Rosen, O.M. Siberian Craton: tectonic zoning, evolution problems. *Geotectonics* **2003**, *3*, 1-19.
69. *Tectonic Map of the Siberian Platform (1:1 500 000), Explanatory note*; Malich, N.S., Tuganova, E.V., Mironyuk, E.P., Eds.; VSEGEI: Leningrad, USSR, 1980; 193 p.
70. Meyer, B.; Saltus, R.; Chulliat, A. *EMAG2v3: Earth Magnetic Anomaly Grid (2-Arc-Minute Resolution)*, 3th ed.; NOAA National Centers for Environmental Information, 2017.
71. Andersen, O.B.; Knudsen, P. Deriving the DTU15 Global high resolution marine gravity field from satellite altimetry. In Proceedings ESA Living Planet Symposium, Prague, Czech Republic, 9-13 May 2016.
72. Vernikovsky, V.A.; Kazansky, A.Y.; Matushkin, N.Y.; Metelkin, D.V.; Sovetov, Y.K. Geodynamic evolution of folding and the western boundary of Siberian Craton into Neoproterozoic: geological and structural, sedimentological, geochronological and paleomagnetic data. *Russ. Geol. Geophys*.; **2009**, *50*, 502-519.
73. Polyansky, O.P.; Reverdatto, V.V.; Ananyev, V.A. Evolution of the rift sedimentary basin as an indicator of the geodynamic situation (Yenisei-Khatanga trough case). *Dokl. Earth Sci*. **2000**, *370*, 71-75.
74. Panin, V.E.; Likhachev, V.A.; Grinyaev, Y.V. *Structural Levels of Deformation of Solid Bodies*; Publishing House Nauka: Novosibirsk, Russia, 1985; 229 p.
75. Konstantinov, K.M.; Bazhenov, M.L.; Fetisova, A.M.; Khutorskoy, D. Paleomagnetism of trap intrusion, East Siberia: implication to flood basalt emplacement and Permo – Triassic crisis of biosphere. *Earth Planet. Sci. Lett.* **2014**, *394*, 242-253.
76. Sharapov, V.N.; Symbireva, I.G.; Bondarenko, P.M. Seismotectonics of the Kurile-Kamchatka Region and its Junction with the Aleutian Arc: Seismological and Tectonophysical Models; Publishing House SB RAS: Novosibirsk, Russia, 1992; 163 p.
77. Kontorovich, A.E.; Belyaev, S.Y.; Kontorovich, A.A.; Krasavchikov, V.O.; Mandelbaum, M.M.; S.A.; Moiseev, A.F.; Safronov, V.S.; Sitnikov, A.V.; Khomenko, Y.G.; Eremin, O.V. Bykova. Tectonics of Vendian-Silurian structural unit of a sedimentary cover of the Lena-Tunguska province of the Siberian Craton. *Russ. Geol. Geophys*. **2009**, *50*, 851–862.
78. *Structural Geology and Plate Tectonics*; Seifert, K.K., Ed.; Publishing House Mir: Moscow, Russia, 1991; Volume 3, 350 p.
79. *Structural Geology and Plate Tectonics*; Seifert, K.K., Ed.; Publishing House Mir: Moscow, Russia, 1991; Volume 1-2, 691 p.
80. *Volcanism in Hawaii*; Decker, R.W., Wright, T.L., Stauffer, P.H., Eds.; US Geological Survey Professional Paper 1350: Washington, USA, 1987; Volume 2, pp. 1667.
81. Sharapov, V.N.; Cherepanov, A.N.; Popov, V.N.; Rakhmenkulova, I.F. Shield volcanoes of Siberian flood basalts: dynamics of lava sheets formation. *Horizons Earth Sci. Res*. **2011**, *4*, 61–98.
82. Kutolin, V.A. *Statistical Study of Basalt Chemistry*; Nauka: Moscow, Russia, 1969; 142 p.
83. Lebedev, S.; van der Hilst, R.D. Global upper-mantle tomography with the automated multimode inversion of surface and S-wave forms. *Geophys. J. Int.*, **2008**, *173*, 505–518.
84. Kuskov, O.L.; Kronred, V.A.; Prokofiev, A.A.; Pavlenkova, N.I. Petroleum-geophysical models of the internal structure of the Siberian Craton lithospheric mantle. *Petrology*, **2014**, *55*, 3-21.
85. Kuskov, O.L.; Kronred, V.A.; Prokofiev, A.A.; Pavlenkova, N.I. Structure of the lithospheric mantle of the Siberian Craton according to the ultra-long seismic profiles Meteorite and Rift. *Russ. Geol. Geophys*. **2014**, *55*, 1124-1143.

 doi:10.20944/preprints202203.0045.v1

86. Ashchepkov, I.V.; Ivanov, A.S.; Kostrovitsky, S.I.; Vavilov, M.A.; Babaurina, S.A.; Vladykin, N.I.; Tychkov, N.S.; Medvedev, N.S. Mantle terranes of Siberian Craton: their interaction with plume melts and based on thermobarometry of mantle xenocrysts. *Geodyn. Tectonophys.* **2019**, *10*, 197-245.
87. Belov, S.V.; Lapin, A.V.; Tolstov, A.V.; Frolov, A.A. *Minerageny of Platform Magmatism (Traps, Carbonatites, Kimberlites)*; SB RAS Publishing: Novosibirsk, Russia, 2008; 537 p.
88. Mehcheryakov, K.A.; Karaseva, T.V. Features of formation of Triassic troughs of the northern West Siberia in connection with petroleum content. *Petrol. Geol. Theor. Appl. Stud.* **2010**, *5*, 1-11.
89. Panin, V.E. Fundamentals of physical mesomechanics. *Phys. Mesomech.* **1998**, *1*, 5–22.
90. Buslov, M.M.; Safonov, I.Y.; Fedoseev, G.S.; Reikov, M.; Davis, K.; Babin, G.A. Permo-Triassic plume magmatism of the Kuznetsk basin (central Asia): geology, geochronology and geochemistry. *Russ. Geol. Geophys*. **2010**, *51*, 1310-1328.
91. Nastavko, A.V.; Borodina, E.V.; Isokh, A.E. Petroleum-mineralogical features of igneous rocks of the central Kuzbass (Southern Siberia). *Russ. Geol. Geophys*. **2012**, *53*, 435-449.
92. Sharapov, V.N.; Vasiliev, Y.R.; Prusskaya, S.N. Petrochemical characteristics of intrusive traps of the western Siberian Platform and the regional zoning of their composition. *Russ. Geol. Geophys*. **2001**, *42*, 1299-1313.
93. Sharapov, V.N.; Vasiliev, Y.R.; Almukhamedov, A.I.; Medvedev, A.Y. On local and regional variability in the composition of Permo-Triassic igneous traps of the Siberian Platform. *Russ. Geol. Geophys*. **2003**, *44*, 741-752.
94. Wooden, J.L.; Czamanske, G.K.; Fedorenko, V.A.; Arndt, N.C.; Chauvel, C.; Bouse, R.M.; King, B-S.W.; Knight, R.J.; Siems, D.F. Isotopic and trace-element constraints on mantle and crustal contributions to Siberian continental flood basalts, Norilsk area, Siberia. *Geochim. Cosm. Acta* **1993**, *57*, 3677-3704.
95. Sharma, M. Siberian traps. In *Large Igneous Provinces: Continental, Oceanic and Planetary Flood Volcanism*; Mahoney, J.J., Coffin, M.F., Eds.; American Geophysical Union Publishing: USA, 1997; Volume 100, pp. 273-295.
96. Sobolev, S.V.; Sobolev, A.V.; Kuzmin, D.V.; Krivolutskaya, N. Linking mantle plumes, large igneous provinces and environmental catastrophes. *Nature* **2011**, *477*, 312-316.